

Multiplexing heralded single-photon in orbital angular momentum space

Shilong Liu,¹ Qiang Zhou,^{2,1,*} Zhiyuan Zhou,^{1,3,†} Shikai Liu,¹
Yinhai Li,¹ Yan Li,¹ Guangcan Guo,^{1,2,3} and Baosen Shi^{1,3,‡}

¹Key Laboratory of Quantum Information, University of Science and Technology of China, Hefei, Anhui 230026, China; and Synergetic Innovation Center of Quantum Information & Quantum Physics, University of Science and Technology of China, Hefei, Anhui 230026, China

²Institute of Fundamental and Frontier Science, University of Electronic Science and Technology of China, Chengdu 610054, China; and School of Optoelectronic Science and Engineering, University of Electronic Science and Technology of China, Chengdu 610054, China

³Heilongjiang Provincial Key Laboratory of Quantum Regulation and Control, Wang Da-Heng Collaborative Innovation Center, Harbin University of Science and Technology, Harbin 150080, China.

(Dated: September 3, 2022)

Heralded single-photon source (HSPS) with competitive single photon purity and indistinguishability has become an essential resource for photonic quantum information processing. Here, for the first time, we proposed and demonstrated a method to generate heralded single-photons by multiplexing the degree of the freedom of orbital angular momentum (OAM) of down-converted entangled photon pairs emitted from a nonlinear crystal. Through multiplexing three OAM modes, the heralded single photon rate obtain a 47% enhancement compared to that with only an individual Gaussian mode. A small value of second-order autocorrelation function $g^{(2)}(0)$ ensures our multiplexed heralded single photons with good single photon purity. We further indicate that an OAM-multiplexed HSPS with high quality can be constructed by generating higher dimensional entangled state and sorting them with high efficiency in OAM space. Our avenue can approach a good HSPS with deterministic property.

Introduction—Perfect single photon source, i.e., emitting indistinguishable single photon on-demand, is a fundamental element for realizing the quantum information processing, such as linear quantum computations [1–3], cryptography [4], and metrology [5]. In the last several decades, much exciting progress has been made to develop such a source. For instance, we try to find suitable platform for deterministic single photon source [6], including quantum dots [7, 8], color centers in diamond or 2D materials [6, 9], and molecules or atoms [10, 11]. Furthermore, we intend to obtain high-quality heralded single-photon source (HSPS) by multiplexing certain degrees of the freedom of photon [12, 13].

For multiplexed HSPS, an essential resource is entangled photon pairs emitted from nonlinear materials, for instance, processes of spontaneous parametric down-conversion (SPDC) and spontaneous four-wave mixing. Based on two types of nonlinear processes, many multiplexed HSPSs with high indistinguishability have been demonstrated in various degrees of the freedom of photon [14], such as in spatial [15–17], temporal [18, 19], polarization [20], spectral [21, 22], and in both spatial and temporal [23–25]. For spatial multiplexing HSPS, the strategy is using multiple basic units to generate photon pairs in different spatial paths, i.e., arrayed silicon waveguides [15], bulk crystals [12] and fibres [16], then multiplexing them into a single path with the help of optical switch. The higher rate of the heralded single photon, the more basic units are needed, resulting in poor scalability. Temporal multiplexing technology with one basic unit has good scalability. However, a successful manip-

ulation requires complex timing sequence [18] and also sacrifices the repetition rate. Another scheme with one basic unit is multiplexing in spectral mode [21, 22]. It is a very promising scheme to develop multiplexed HSPS approaching to a deterministic single photon source, while manipulating spectral modes needs robust optical filtering otherwise very noisy [22], or the performance of frequency shifting devices limit the number of modes [21]. Therefore, it is a valuable direction to explore an unique high-performance HSPS with a single basic unit multiplexed in new degree of the freedom of photon.

Recently, orbital angular momentum (OAM), a remarkable degree of freedom of photon with infinite dimensions, has obtained increasing attention and rapid development [26–28]. High-dimensional photonic state encoded with vortex wavefront ($e^{iL\phi}$) can increase the capacity of carrying information, which is natural and quite essential for scalability in classical and quantum information applications [29, 30]. In the field of quantum information, much progress of high-dimensional quantum state has been achieved [27, 28], such as realizing multilevel quantum systems [31], generating a high-dimensional maximally entangled state [32–34], and exploring the high-dimensional quantum computations, i.e., high-dimensional single-photon gate [35] and Bell basis [36]. Towards generating a high-dimensional entangled state in OAM space for multiplexed HSPS, the most common method is to engineer down concerted photon pairs emitted from a nonlinear crystal through the process of SPDC [31]. The spatially entangled down-converted photon pairs in SPDC can be written as

$\sum_{L_s, P_s} \sum_{L_i, P_i} c_{P_s, P_i}^{L_s, L_i} |L_s, P_s\rangle |L_i, P_i\rangle$ in Laguerre-Gauss mode basis [37], where the indices of $L_{s(i)}$ and $P_{s(i)}$ described the azimuthal and radial OAM modes; $|c_{P_s, P_i}^{L_s, L_i}|^2$ represents a coincidence probability for finding one signal photon in spatial modes of L_s, P_s and one idler photon in spatial modes of L_i, P_i . Because the radial value of P between pumps and down-converted photon pairs are not conserved [38], we only consider the azimuthal values of L . According to the OAM conservation between signal, idler and pump photons, i.e. $L_p = L_s + L_i$, the output state can be written as $\sum_{L=-\infty}^{\infty} c_L |L\rangle_s |-L\rangle_i$, where the distribution of amplitudes c_L associates with the spiral bandwidth of entangled two-photon state, which usually rapidly decreases as the increase of topological number of OAM [37]. Previous works on multiplexed HSPS always focus on parts of zero state, or Gaussian beam, and neglect the occupations of high orders in OAM space. In most situation, we cannot ignore the amplitude of $c_L (|L| \neq 0)$, for example, the amplitudes of $c_{\pm 1}$ near the zero order have a considerable value [37]. Therefore a high-efficiency and well scalable multiplexed HSPS would be developed if the high-order OAM parts employed in such system.

In this letter, we propose and demonstrate a multiplexed HSPS in the OAM degree of freedom of the photon. First, we describe the fundamental principle of constructing an HSPS by multiplexing the OAM entangled photon pairs in the SPDC process. Then, a proof-of-principle multiplexed HSPS is demonstrated by multiplexing three OAM modes: $c_{-1} |-1\rangle_s |1\rangle_i + c_0 |0\rangle_s |0\rangle_i + c_1 |1\rangle_s |-1\rangle_i$. Finally, we make a discussion about the OAM-HSPS. In our experiment, the enhancement is up to 47% compared to the only one Gaussian mode. To verify that the OAM-HSPS is indeed in the single-photon regime, we carry out the Hanbury Brown and Twiss (HBT) experiment to measure the second-order autocorrelation function $g^{(2)}(\tau)$. A smaller $g^{(2)}(0)$ indicates a higher single photon purity [39, 40]. We obtained the value of $g^{(2)}(0) = 0.097 \pm 0.011$ for OAM-HSPS. The results in our experiment illustrate that the OAM-HSPS is of good quality and is a promising avenue for single photon-source.

Principle. The principle for OAM-HSPS is shown in Figure 1. By considering the azimuthal variable of L , the state of entangled photon pairs from the process of SPDC can be written as $\sum_{L=-\infty}^{\infty} c_L |L\rangle_s |-L\rangle_i$ [37]. The state of $|L\rangle_s |-L\rangle_i$ represents one signal photon in the spatial mode of L_s and another idler photon in the spatial mode of $-L_i$. The photon pairs can be separated into two paths by using a polarization beam splitter (PBS) in experiment. A simple picture is shown in Fig. 1(b), where the idler photons are heralding photons, and the signal photons are heralded ones. The idler photons are sorted to one of the paths based on the value of $-L_i$ by an OAM-sorter. Later, the idler photon $|-L_i\rangle_i$ is detected

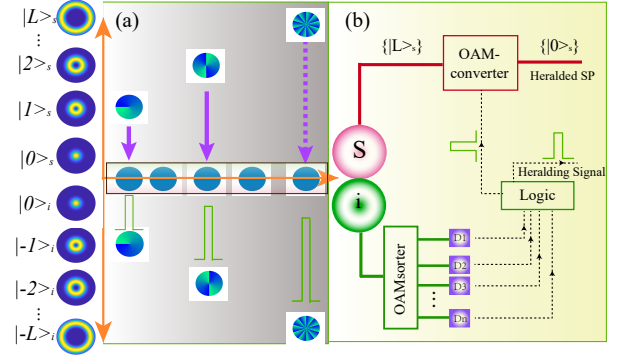


FIG. 1. The principle of the OAM-HSPS. a, the schematic of multiplexing OAM modes. b, the simple regime for OAM-HSPS. High-dimensional entangled photon pairs (signal and idler photons) are from the process of SPDC. The state $|L\rangle_s$ of signal photon will be converted instantly to a signal photon without vortex phase triggering by the heralding signal.

by a single photon detector (D_n) for generating a heralding electronic signal. In the meantime, the entangled signal photon $|L\rangle_s$ arrive at an OAM-converter, which is on-demand controlled by the heralding electronic signal; after passing through the OAM-converter, the vortex phase $\exp(iL_s\phi)$ of the signal photon is converted instantly to a plane phase ($L_s = 0$) for detections. Fig. 1(a), a simplified diagram, shows the schematic of the OAM-HSPS. By adding more and more OAM modes, the heralded photons will yield a considerable improvement compared with the only Gaussian mode. In the overall process of the multiplexing, two essential elements, i.e., an OAM-sorter with high-efficiency and an OAM-converter with high-speed, are needed. Many OAM-sorters have been demonstrated, such as Mach-Zehnder interferometers-based [41] and spatial light modulators-based [27, 42]. We have to use numerous optical elements for separating three OAM modes if we employ the interferometric methods in Ref. [41], which is not suitable in this experiment. By performing a Cartesian to log-polar coordinate transformation [42], we can efficiently sort several OAM modes. However, we need even three SLMs and the global sorting efficiency will be reduced. An OAM-sorter with high-efficiency and sorting as many as possible modes is still missing. Meanwhile, the performance of OAM-converter is also far from perfect. For instance, the input frame rate of the commercial SLM is limited to several hundred Hertz. Although the employed OAM-sorters and -converters are not ideal, we demonstrate a proof-of-principle experiment for OAM-HSPS in our work.

The experimental setup with methods being equivalent to OAM-sorting and -converting functions is presented in Fig. 2. Photon pairs occupied in three OAM modes are utilized, i.e., $c_{-1} |-1\rangle_s |1\rangle_i$, $c_0 |0\rangle_s |0\rangle_i$, $c_1 |1\rangle_s |-1\rangle_i$. For the heralding side, the OAM-sorter, including a SLM-

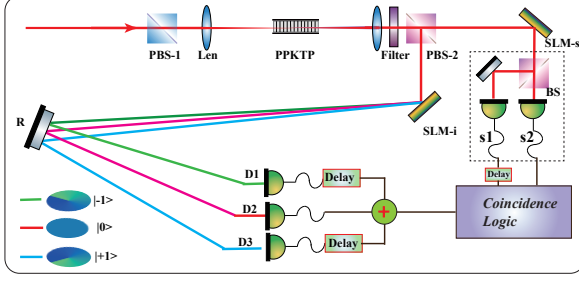


FIG. 2. Schematics for OAM-HSPS. A narrow bandwidth 780 nm laser beam (Ti: sapphire, MBR110, Coherent) pumps a type-II Periodically Poled Potassium Titanyl Phosphate (PPKTP, $1 \times 2 \times 10 \text{ mm}^3$). The beam of signal and idler photons in the center of PPKTP are exactly imaged on the planes of two spatial light modulators (SLMs), i.e. SLM-s and SLM-i, by using a convex lens. Signal and idler photons are separated by a polarization beam splitter (PBS). Both SLM-s and SLM-i are encoded with complex opposite phases. The path of the signal is the heralded port, where we use a projection measurement superposition state $|1\rangle + |0\rangle + |-1\rangle$ to sharp the corresponding vortex phase. The idler is the heralding port, where the projection measurement states are analogous to the signals with a different blazed grating constant for three basic OAM modes.

i , is used to convert three OAM modes into three different spatial Gaussian modes. After the mode sorting, the modes $|-1\rangle_i$, $|0\rangle_i$ and $|1\rangle_i$ are detected by three single photon detectors, i.e., D1, D2, and D3, respectively. The OAM mode-sorting is realized by loading a complex phase of $\text{Arg}(e^{1 \times \psi})e^{ikd_{-1}} + \text{Arg}(e^{0 \times \psi})e^{ikd_0} + \text{Arg}(e^{-1 \times \psi})e^{ikd_1}$ onto the SLM-i, where the phase of $\text{Arg}(e^{-L_i \times \psi})$ is used to flat the vortex phase of the input photon; $e^{ikd_{L_i}}$ represents a displacement operation for the OAM mode of $|L_i\rangle$ [43, 44]. What we need to pay attention to is the above method exist an efficiency of $1/3$ for one of input modes, for example, the state will be $|0\rangle_{D1} + |-1\rangle_{D2} + |-2\rangle_{D3}$ if the input state is $|-1\rangle_i$. For the heralded side, we employ a SLM-s to realize the function of the OAM-converter, where the acquired phase is similar to the situation of OAM-sorter beside the displacement operation, $d_{L_s} = 0$. After passing through the OAM-converter, all of the modes $|L\rangle_s$ of signal photon is converted to $|0\rangle_s$ with a probability of $1/3$, and mode $|0\rangle_s$ is filtered and collected by using a single mode fiber.

Results. Considering three OAM modes, the quantum state of down-converted pairs can be written as $c_{-1}|-1\rangle_s|1\rangle_i + c_0|0\rangle_s|0\rangle_i + c_1|1\rangle_s|-1\rangle_i$. The coincidence rate for each OAM entangled mode is proportional to the coefficient c_0^2 or $c_{\pm 1}^2$. By multiplexing three OAM modes, the enhancement can be improved of $1 + 2\xi^2$ in contrast to a single Gaussian mode, where $\xi = |c_1|/|c_0|$ represents the scale of enhancement, for example, for the case with only Gaussian mode, there is no enhancement due to $\xi = 0$; for the three-dimensional maximum entanglement

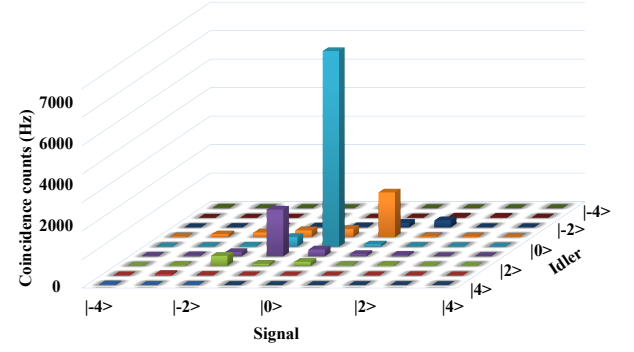


FIG. 3. The spatial distributions of down-converted photon pairs, where the pump is a Gaussian beam, two SLMs load the corresponding OAM-eigen state of the pure phase. Each coincidence is measured in one second.

state [45], all the amplitudes is equally ($|c_{\pm 1}| = |c_0|$), and the enhancement is up to 3; higher dimension corresponds to a higher rate of HSPS. In our experiment, the value of ξ^2 is 0.446, which can be measured by the spatial distributions of down-converted photons. Figure 3 shown the results for the spatial distributions of down-converted photons in OAM space, where $x(y)$ -axis represents the pure OAM eigen states from -4 to 4; z axis is the coincidence recorded in one second.

To verify that the output OAM-HSPS maintains the single-photon characters, we measured the second-order autocorrelation function $g^{(2)}(\tau) = C_{s_1, s_2, i}(\tau) \cdot C_i / C_{i, s_1}(\tau) \cdot C_{i, s_2}(0)$ of single and after multiplexing sources. Here, $C_{s_1, s_2, i}(\tau)$ is the three-fold coincidence between the signal of s_1 and s_2 separated by a beam splitter (the dashed box in Fig. 2) and the idler of i ; $C_{i, s_1}(\tau)$ and $C_{i, s_2}(0)$ represent two-fold coincidences between idler and s_1 , and s_2 , respectively; C_i is the number of clicks of idler, the heralding counts. τ is the delay between heralded s_1 and heralding i , which is usually on a magnitude of nanoseconds [40]. In principle, the lower values of $g^{(2)}(0)$ is, the higher purity of the single photon source is. To measure $g^{(2)}(\tau)$, we employ the most common method, Hanbury-Brown and Twiss (HBT) setups [39]. In our setups, the components in the dashed box shown in Fig. 2 are the HBT setups for measuring the property of the heralded photons. First, we measure the $g^{(2)}(\tau)$ for the single OAM modes, where the phases encoded in SLM-s/SLM-i are $|1\rangle_s / |-1\rangle_i$, $|0\rangle_s / |0\rangle_i$, and $|-1\rangle_s / |1\rangle_i$, respectively. The obtained $g^{(2)}(0)$ is shown by orange coloured bars in the Fig. 4(c), and the overall measurements of $g^{(2)}(\tau)$ for $|0\rangle_s / |0\rangle_i$ is plotted in the Fig. 4(a). Here, the x-axis is the delays and the coincidence windows is 1.6 ns in our experiments. Then, we measure the $g^{(2)}(0)$ of the OAM-HSPS. Here, the phases for two SLMs are $|1\rangle_s + |0\rangle_s + |-1\rangle_s$ and $|-1\rangle_i e^{ikd_{-1}} + |0\rangle_i e^{ikd_0} + |1\rangle_i e^{ikd_1}$. The corresponding values of $g^{(2)}(0)$ are plotted by blue coloured bars in Fig. 4(c). Be-

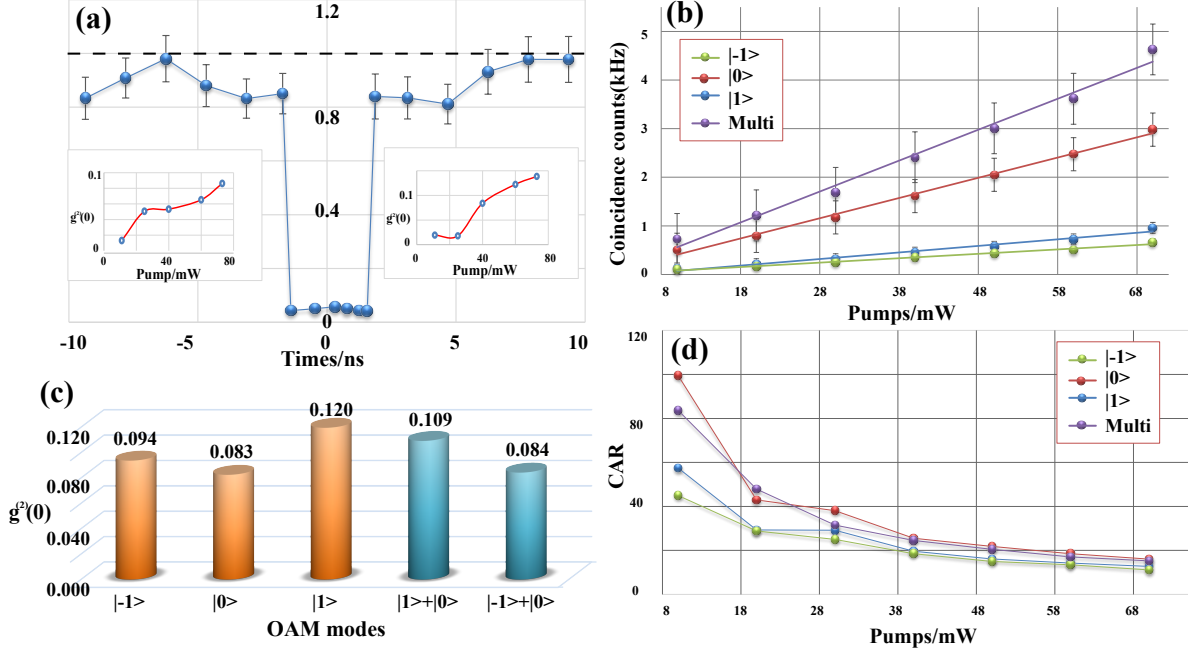


FIG. 4. The results of second-order autocorrelation function $g^{(2)}(\tau)$ and rates of the single and multiplexing OAM-HSPS. a: The distributions $g^{(2)}(\tau)$ of $|0\rangle_s/|0\rangle_i$; where error bars are estimated using Poisson statistics; the measured average $g^{(2)}(0) = 0.048 \pm 0.003$ c: The average $g^{(2)}(0)$ for single or OAM-HSPS. The coincidences during the measurement of $g^{(2)}(\tau)$ are recorded over 40 seconds, and the pump is the Gaussian beam with the power of 77 mW. The average measured second-order autocorrelation function $g^{(2)}(0) = 0.094 \pm 0.017, 0.083 \pm 0.008, 0.120 \pm 0.019, 0.109 \pm 0.012, \text{ and } 0.084 \pm 0.009$ for single and multi modes. b: The Heralded single-photon rates from OAM modes of $|-1\rangle$ (green dot), $|0\rangle$ (red dot), $|1\rangle$ (blue dot), and after multiplexing (purple dot) are plotted as a range of input powers, d: The CAR obtained from the same conditions of a. Lines are linear fits to the data, here, the coincidences in the measurement of rate are recorded 20 seconds.

cause of the different collected efficiency between mode of $|1\rangle$ and $|-1\rangle$ during the measurement, the measured $g^{(2)}(0)$ of $|1\rangle + |0\rangle$ is a bit higher than the situation of $|-1\rangle + |0\rangle$. Nevertheless, all the measured values of $g^{(2)}(0)$ are around 0.1, which shows the OAM-HSPS with good single photon purity and close to true single photon source. Finally, we measure the value of $g^{(2)}(0)$ of OAM-HSPS with the increase of pump power, which are inserted in Fig. 4(a), where the OAM-HSPS with two OAM modes, $|-1\rangle + |0\rangle$, is the left one, and with $|1\rangle + |0\rangle$ is the right one, respectively.

In addition, we measure the OAM-HSPS rates with various pump powers. These results are plotted in Fig. 4(b), where green, red, and blue dots show the coincidence with the modes of $|-1\rangle_i|1\rangle_s$, $|0\rangle_i|0\rangle_s$, and $|1\rangle_i|1\rangle_s$, respectively; the purple one gives the result of OAM-HSPS after multiplexing. Based on four fitting curves, we can infer the enhancement of HSPS with three OAM modes of 1.47, or 47% increase, which is lower than the theories where the enhancement should be 1.89 for our system ($\xi^2 = 0.446$). The main reason is that the asymmetrical losses between Gaussian and high-order modes during the projection measurements.

Due to this type of OAM converter, the current OAM-

HSPS rates for signal port is with a efficiency around 30%. The overall OAM-HSPS rates can be improved in further if we decrease the losses of transmission and sorting, i.e. developing an OAM-sorter/OAM-converter with higher efficiency. Nevertheless, as a proof-of-principle demonstration, we realize successfully the enhancement by multiplexing three OAM modes. Furthermore, we measured the coincidence-to-accidental coincidence ratio (CAR), a standard signal-to-noise metric for probabilistic photon pairs. The corresponding CAR is depicted in Fig. 4(d), where the colours of data represent as the same meaning as in Fig. 4(b). Similar with the result of another multiplexing systems [15, 16], the CAR has a rapid decrease as the increase of pump power in our systems.

We did not directly measure the distinguishability of single photons from our source, but in our experimental setup, we conjecture that they must be nearly indistinguishable. Because all the vortex photon with non-Gaussian transverse mode structure is converted into the Gaussian mode, i.e., $\{|-1\rangle, |0\rangle, |1\rangle\} \rightarrow \{|0\rangle, |0\rangle, |0\rangle\}$, we can't distinguish definitely where the photon state $|0\rangle$ come from each of pair. The principle of distinguishability is the same as other degree of the freedom of the

photon.

Discussion. We firstly demonstrated an HSPS by multiplexing the multi-mode of down-converted photon pairs emitted from the nonlinear crystal in the process of SPDC. The photon rate of OAM-HSPS obtained a considerable enhancement of 47% by multiplexing three OAM modes. A conditional second-order autocorrelation function value $g^{(2)}(0)$ close to 0.1, illustrates that the generated photons are with high single photon purity. The enhancement can be improved in further if we decrease the overall losses in the system. The losses of the system, mainly caused by the OAM sorting and converting method employed in our experiment, limit the overall HSPS rate. Nevertheless, the overall losses do not affect the enhancement of multiplexing OAM modes in principle. Our proof-of-principle OAM-HSPS shown that we can construct a good HSPS by multiplexing more OAM modes, i.e., by multiplexing high-dimensional entangled state in OAM space [32], or high-dimensional maximally entangled state [45–47]. Recently, we realized an arbitrary superposition state of even 50 OAM modes, an analogous OAM-Schrödinger cat state in Ref [48], so this platform for OAM-HSPS is with excellent scalability. We believe that our works can be considered an important first step towards reaching a high-quality and well-scalability HSPS. We hope that our work will inspire further research in this direction. The unsolved challenges are to implement a lossless OAM-sorter working with as more as possible OAM modes. Because the manipulation of a lossless OAM-sorter is still a well-defined problem, it has a great potential for development of a highly efficient OAM-based HSPS.

Acknowledgments This work is partially supported the Anhui Initiative in Quantum Information Technologies (AHY020200); National Key R&D Program of China (2018YFA0307400); National Natural Science Foundation of China (61435011, 61525504, 61605194, 61775025, 61405030); China Postdoctoral Science Foundation (2016M590570, 2017M622003); Fundamental Research Funds for the Central Universities.

* zhouqiang@uestc.edu.cn

† zyzhouphy@ustc.edu.cn

‡ drshi@ustc.edu.cn

- [1] N. Gisin, G. Ribordy, W. Tittel, and H. Zbinden, *Rev. Mod. Phys.* **74**, 145 (2002).
- [2] E. Knill, R. Laflamme, and G. J. Milburn, *Nature* **409**, 46 (2001).
- [3] T. D. Ladd, F. Jelezko, R. Laflamme, Y. Nakamura, C. Monroe, and J. L. O'Brien, *Nature* **464**, 45 (2010).
- [4] C. H. Bennett and G. Brassard, *Theor. Comput. Sci.* **560**, 7 (2014).
- [5] V. Giovannetti, S. Lloyd, and L. Maccone, *Phys. Rev. Lett.* **96**, 010401 (2006).
- [6] I. Aharonovich, D. Englund, and M. Toth, *Nat. Photonics* **10**, 631 (2016).
- [7] X. Ding, Y. He, Z.-C. Duan, N. Gregersen, M.-C. Chen, S. Unsleber, S. Maier, C. Schneider, M. Kamp, S. Höfling, *et al.*, *Phys. Rev. Lett.* **116**, 020401 (2016).
- [8] N. Somaschi, V. Giesz, L. De Santis, J. Loredano, M. P. Almeida, G. Hornecker, S. L. Portalupi, T. Grange, C. Antón, J. Demory, *et al.*, *Nat. Photonics* **10**, 340 (2016).
- [9] C. Kurtsiefer, S. Mayer, P. Zarda, and H. Weinfurter, *Phys. Rev. Lett.* **85**, 290 (2000).
- [10] B. Lounis and W. E. Moerner, *Nature* **407**, 491 (2000).
- [11] C. Chou, S. Polyakov, A. Kuzmich, and H. Kimble, *Phys. Rev. Lett.* **92**, 213601 (2004).
- [12] A. L. Migdall, D. Branning, and S. Castelletto, *Phys. Rev. A* **66**, 053805 (2002).
- [13] T. Pittman, B. Jacobs, and J. Franson, *Phys. Rev. A* **66**, 042303 (2002).
- [14] R. J. Francis-Jones, *Active Multiplexing of Spectrally Engineered Heralded Single Photons in an Integrated Fibre Architecture* (Springer, 2017).
- [15] M. J. Collins, C. Xiong, I. H. Rey, T. D. Vo, J. He, S. Shahnia, C. Reardon, T. F. Krauss, M. Steel, A. S. Clark, *et al.*, *Nat. Commun.* **4**, 2582 (2013).
- [16] R. J. Francis-Jones, R. A. Hoggarth, and P. J. Mosley, *Optica* **3**, 1270 (2016).
- [17] L. Mazzarella, F. Ticozzi, A. V. Sergienko, G. Vallone, and P. Villoresi, *Phys. Rev. A* **88**, 023848 (2013).
- [18] F. Kaneda, B. G. Christensen, J. J. Wong, H. S. Park, K. T. McCusker, and P. G. Kwiat, *Optica* **2**, 1010 (2015).
- [19] C. Xiong, X. Zhang, Z. Liu, M. J. Collins, A. Mahendra, L. Helt, M. Steel, D.-Y. Choi, C. Chae, P. Leong, *et al.*, *Nat. Commun.* **7**, 10853 (2016).
- [20] X.-S. Ma, S. Zotter, J. Kofler, T. Jennewein, and A. Zeilinger, *Phys. Rev. A* **83**, 043814 (2011).
- [21] M. G. Puigibert, G. Aguilar, Q. Zhou, F. Marsili, M. Shaw, V. Verma, S. Nam, D. Oblak, and W. Tittel, *Phys. Rev. Lett.* **119**, 083601 (2017).
- [22] C. Joshi, A. Farsi, S. Clemmen, S. Ramelow, and A. L. Gaeta, *Nat. Commun.* **9**, 847 (2018).
- [23] G. J. Mendoza, R. Santagati, J. Munns, E. Hemsley, M. Piekarek, E. Martín-López, G. D. Marshall, D. Bonneau, M. G. Thompson, and J. L. O'Brien, *Optica* **3**, 127 (2016).
- [24] F. Kaneda and P. G. Kwiat, *arXiv preprint arXiv:1803.04803* (2018).
- [25] M. Heuck, M. Pant, and D. R. Englund, *New J. Phys.* (2018).
- [26] L. Allen, M. W. Beijersbergen, R. J. C. Spreeuw, and J. P. Woerdman, *Phys. Rev. A* **45**, 8185 (1992).
- [27] A. M. Yao and M. J. Padgett, *Adv. Opt. Photonics* **3**, 161 (2011).
- [28] M. Erhard, R. Fickler, M. Krenn, and A. Zeilinger, *Light: Science & Applications* **7**, 17146 (2018).
- [29] J. Wang, J.-Y. Yang, I. M. Fazal, N. Ahmed, Y. Yan, H. Huang, Y. Ren, Y. Yue, S. Dolinar, M. Tur, *et al.*, *Nat. Photonics* **6**, 488 (2012).
- [30] N. Bozinovic, Y. Yue, Y. Ren, M. Tur, P. Kristensen, H. Huang, A. E. Willner, and S. Ramachandran, *Science* **340**, 1545 (2013).
- [31] A. Mair, A. Vaziri, G. Weihs, and A. Zeilinger, *Nature* **412**, 313 (2001).
- [32] A. C. Dada, J. Leach, G. S. Buller, M. J. Padgett, and E. Andersson, *Nat. Phys.* **7**, 677 (2011).
- [33] S. Franke-Arnold, S. M. Barnett, E. Yao, J. Leach,

- J. Courtial, and M. Padgett, *New J. Phys.* **6**, 103 (2004).
- [34] M. Malik, M. Erhard, M. Huber, M. Krenn, R. Fickler, and A. Zeilinger, *Nat. Photonics* **10**, 248 (2016).
- [35] A. Babazadeh, M. Erhard, F. Wang, M. Malik, R. Nouroozi, M. Krenn, and A. Zeilinger, *Phys. Rev. Lett.* **119**, 180510 (2017).
- [36] F. Wang, M. Erhard, A. Babazadeh, M. Malik, M. Krenn, and A. Zeilinger, *Optica* **4**, 1462 (2017).
- [37] J. Torres, A. Alexandrescu, and L. Torner, *Phys. Rev. A* **68**, 050301 (2003).
- [38] F. M. Miatto, A. M. Yao, and S. M. Barnett, *Phys. Rev. A* **83**, 033816 (2011).
- [39] R. H. Brown and R. Q. Twiss, *Nature* **177**, 27 (1956).
- [40] E. Bocquillon, C. Couteau, M. Razavi, R. Laflamme, and G. Weihs, *Phys. Rev. A* **79**, 035801 (2009).
- [41] J. Leach, M. J. Padgett, S. M. Barnett, S. Franke-Arnold, and J. Courtial, *Phys. Rev. Lett.* **88**, 257901 (2002).
- [42] G. C. Berkhout, M. P. Lavery, J. Courtial, M. W. Beijersbergen, and M. J. Padgett, *Phys. Rev. Lett.* **105**, 153601 (2010).
- [43] G. Gibson, J. Courtial, M. J. Padgett, M. Vasnetsov, V. Pasko, S. M. Barnett, and S. Franke-Arnold, *Opt. Express* **12**, 5448 (2004).
- [44] S. Li and J. Wang, *Sci. Rep.* **5**, 15406 (2015).
- [45] S.-L. Liu, Z.-Y. Zhou, S.-K. Liu, Y.-H. Li, Y. Li, Z.-h. Xu, Z.-d. Liu, G.-C. Guo, B.-S. Shi, *et al.*, arXiv preprint arXiv:1807.07257 (2018).
- [46] A. Vaziri, G. Weihs, and A. Zeilinger, *Phys. Rev. Lett.* **89**, 240401 (2002).
- [47] E. Kovlakov, S. Straupe, and S. Kulik, arXiv preprint arXiv:1807.09804 (2018).
- [48] S.-L. Liu, Z.-Y. Zhou, Q. Zhou, S.-K. Liu, Y. Li, Y.-H. Li, G.-C. Guo, and B.-S. Shi, arXiv preprint arXiv:1807.05498 (2018).